Journal of civil engineering and transport **transEngin**

2020, Volume **2** Number **3** **ISSN 2658-1698, e-ISSN 2658-2120**

DOI: 10.24136/tren.2020.012

MATHEMATICAL MODELING OF UNMANNED MOVEMENT AIRCRAFT - FOUR-ROTOR

Jerzy **Kisilowski** [1], Rafał **Kowalik** [2,*], Łukasz **Parszutowicz** [3]

[1] University of Technology and Humanities, Faculty of Transport, Electrical Engineering and Computer Science, Malczewskiego 29, 26-600 Radom, Poland, email: jerzy@kisilowscy.waw.pl, https://orcid.org/0000-0003-3747-0578

[2] Department of Avionics and Control Systems, Military University of Aviation, 08-521 Deblin, Poland, e-mail: r.kowalik@law.mil.pl, https://orcid.org/0000-0001-6431-9561

[3] University of Technology and Humanities, Faculty of Transport, Electrical Engineering and Computer Science, Malczewskiego 29, 26-600 Radom, Poland, work master of science

* Corresponding author

Reviewed positively: 15.03.2021

Information about quoting an article:

Kisilowski J., Kowalik R., Parszutowicz Ł. (2020). Mathematical modeling of unmanned movement aircraft - four-rotor. Journal of civil engineering and transport. 2(3), 149-163, ISSN 2658-1698, e-ISSN 2658-2120, DOI: 10.24136/tren.2020.012

Abstract – The article presents an analytical approach to building a mathematical model of a quadrocopter. The main purpose of building the model was to design an appropriate facility control system and analyze its behavior in various situations. The assumption was made to build a model, control system and all accompanying algorithms in an open programming environment, which will allow their subsequent implementation in a real facility, without the need to use expensive software. The quadrocopter is controlled by the operator by means of hand movements that are read by the camera and properly interpreted using advanced image processing methods. The entire system is visualized and embedded in a three-dimensional simulation environment. The model study was conducted using a DC motor as an input data source. The operation of the model was checked with a controller when a disturbance was introduced into the model. The four-rotor model with a selected regulator was tested by analyzing the angular velocity and position of the object in a rectangular coordinate system. At the end of the article, the results of the simulations made are presented and the resulting conclusions are presented.

Key words – quadrocopter, drone, dynamics system, UAV, modelling

JEL Classification – C02, C60, C61, C63

INTRODUCTION

The task of mathematical modeling of a four-rotor (drone) has been the subject of many papers [1-4]. Mathematical models were determined using two rectangular coordinate systems (right-handed system). One is related to the earth XYZ - non-inertial system, and the rectangular coordinate systems related to the four-rotor systems coinciding with the symmetry axes of the elements, on which also the moments of inertia lie - the system called inertial [5], [6], [22], Fig. 1. O_i, X_i, Z_i.

The angular velocity vectors were assumed to lie on the axes of a rectangular coordinate system, which leads to the fact that angles are rotations around the axis of a rectangular coordinate system - often called - heel angle, - tilt angle, - yaw angle. It was assumed that the coordinate systems are shown in Figure 1. The equations of motion were derived using the d'Alembert principle.

1. MATHEMATICAL MODEL OF A FOUR-ROTOR

The mathematical model was determined from the coordinates defined in introduction Chapter.

When building the mathematical model of the quadrocopter, the following assumptions were made:

- the matrix of directional cosines between the non-inertial and inertial systems was adopted as zero-one [5],
- solids are assumed to be rigid,
- the center of gravity of the body and the origin of the reference axis system are assumed to coincide,

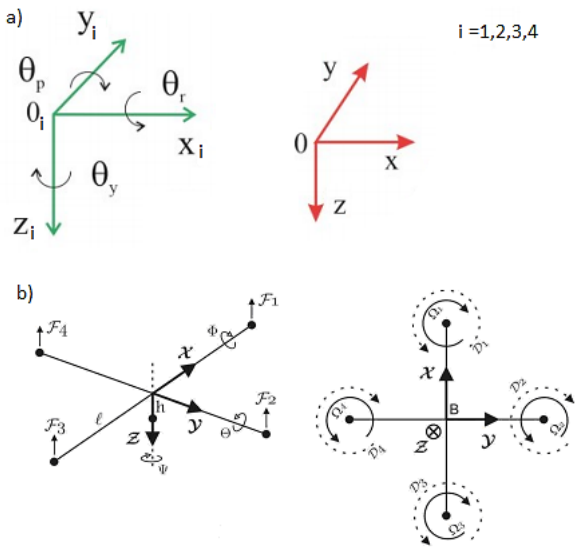

Fig. 1. Coordinate systems adopted in determining the mathematical model

- thrust and drag are proportional to the square of the propeller speed,
- the propellers are to be stiff,
- the structure is to be axially symmetrical.

In order to determine the equations, the forces and moments acting on the four-rotor [3], [10], [11], which are given below, were adopted. J_r is the rotor moment of inertia, T is the thrust, H is the hub force (the sum of the horizontal forces acting on the blade elements), Q is the rotor resistance moment (due to aerodynamic forces), R_m is the rotor rolling moment.

Torques:

- body gyroscopic effect $\dot{\theta}\dot{\psi}(I_{yy} - I_{zz})$
- torque due to forward flight $(-1)^{i+1}\sum_{i=1}^{4} R_{mxi}$
- gyroscopic propeller effect $J_r\dot{\theta}\Omega_r$
- hub moment due to side flight $h\sum_{i-1}^{4} H_{yi}$
- operation of rotary actuators $l(-T_2 + T_4)$ *Tilt moments:*

Moments of deviations:

- body gyroscopic effect $\dot{\theta}\dot{\phi}(I_{xx} - I_{yy})$
- hub force imbalance in forward flight $l(H_{x2} - H_{x4})$
- inertial counter torque $J_r\Omega_r$
- hub force imbalance in side flight $l(-H_{y1} + H_{y3})$
- unbalancing the opposite moment $(-1)^{i}\sum_{i=1}^{4} Q_i$

Forces along the z axis:

- operation of actuators $\cos\psi\cos\phi\sum_{i=1}^{4} T_i$

- weight mg ng the x axis:

Forces along the x axis:

- operation of actuators $(\sin\psi\,\sin\phi + \cos\psi\,\sin\theta\,\cos\phi)\sum_{i=1}^{4} T_i$
- hub force in the x axis $-\sum_{i=1}^{4} H_{xi}$
- friction $\frac{1}{2} C_y A_c \rho \dot{y}|\dot{y}|$

Forces along the y axis:

- operation of actuators $(-\cos\psi\,\sin\phi + \sin\psi\,\sin\theta\,\cos\phi)\sum_{i=1}^{4} T_i$
- hub forces in the *y* axis $-\sum_{i=1}^{4} H_{xi}$
- friction $\frac{1}{2} C_y A_c \rho \dot{y}|\dot{y}|$

where l is the distance between the propeller axis and the center of gravity, h is the vertical distance from the propeller center to the center of gravity, Ω_r is the overall residual angular velocity of the propeller, and I is the rotor moment of inertia.

The equations of motion were derived based on the d'Alembert principle on the basis of publications [12-13]. G is the acceleration of gravity and m is the mass of the quadrocopter.

$$I_{xx}\ddot{\phi} = \dot{\theta}\dot{\psi}\left(I_{yy}I_{zz}\right) + J_r\dot{\theta}\Omega_r + l(-T_2 + T_4) - h\sum_{i=1}^{4} H_{yi} + (-1)^{i+1}\sum_{i=1}^{4} R_{mxi} \quad (1)$$

$$I_{yy}\ddot{\theta} = \dot{\phi}\dot{\psi}(I_{zz}I_{xx}) - J_r\dot{\theta}\Omega_r + l(-T_1 + T_3) + h\sum_{i=1}^{4} H_{xi} + (-1)^{i+1}\sum_{i=1}^{4} R_{myi} \quad (2)$$

$$I_{zz}\ddot{\psi} = \dot{\theta}\dot{\phi}\left(I_{xx}I_{yy}\right) + J_r\Omega_r + l\left(H_{x2} - H_{x4}\right) + l\left(-H_{y1} + H_{y3}\right) + (-1)^{i}\sum_{i=1}^{4} Q_i \quad (3)$$

$$m\ddot{z} = mg - (\cos\psi\cos\phi)\sum_{i=1}^{4} T_i \quad (4)$$

$$m\ddot{x} = (\sin\phi\sin\psi + \cos\psi\sin\theta\cos\phi)\sum_{i=1}^{4} T_i - \sum_{i=1}^{4} H_{xi} \quad (5)$$

$$m\ddot{y} = (-\sin\phi\cos\psi + \sin\psi\sin\theta\cos\phi)\sum_{i=1}^{4} T_i - \sum_{i=1}^{4} H_{yi} \quad (6)$$

The main aerodynamic forces and moments acting on a four-rotor during the hover segment correspond to thrust (T), hub force (H) and drag torque (Q) due to vertical, horizontal and aerodynamic forces, respectively, and the torque (R) associated with integrating the lift force of all rotors operating at a given radius [11]. The extended formulation of these forces and moments can be found in [12-13]. The nonlinear dynamics of the system is described by the following equations [4]:

$$\dot{X} = \begin{vmatrix} \dot{\phi} \\ \ddot{\phi} \\ \dot{\theta} \\ \ddot{\theta} \\ \dot{\psi} \\ \ddot{\psi} \\ \dot{z} \\ \ddot{z} \\ \dot{x} \\ \ddot{x} \\ \dot{y} \\ \ddot{y} \end{vmatrix} = \begin{vmatrix} \dot{\phi} \\ \dot{\theta}\dot{\psi}\dfrac{I_{yy} - I_{zz}}{I_{xx}} + \dfrac{l_a}{I_{xx}}U_2 \\ \dot{\theta} \\ \dot{\theta}\dot{\psi}\dfrac{I_{zz} - I_{xx}}{I_{yy}} + \dfrac{l_a}{I_{yy}}U_3 \\ \dot{\psi} \\ \dot{\theta}\dot{\phi}\dfrac{I_{xx} - I_{yy}}{I_{zz}} + \dfrac{1}{I_{zz}}U_4 \\ \dot{z} \\ g - (\cos\phi\cos\theta)\dfrac{U_1}{m_s} \\ \dot{x} \\ u_x\dfrac{U_1}{m_s} \\ \dot{y} \\ u_y\dfrac{U_1}{m_s} \end{vmatrix} + \begin{vmatrix} 0 \\ W_1 \\ 0 \\ W_2 \\ 0 \\ W_3 \\ 0 \\ W_4 \\ 0 \\ W_5 \\ 0 \\ W_6 \end{vmatrix} \tag{7}$$

$$U = \begin{vmatrix} U_1 \\ U_2 \\ U_3 \\ U_4 \end{vmatrix} = \begin{vmatrix} b(\Omega_1^2 + \Omega_2^2 + \Omega_3^2 + \Omega_4^2) \\ b(-\Omega_2^2 + \Omega_4^2) \\ b(\Omega_1^2 - \Omega_3^2) \\ d(-\Omega_1^2 + \Omega_2^2 - \Omega_3^2 + \Omega_4^2) \end{vmatrix} \tag{8}$$

$$\begin{vmatrix} u_x \\ u_y \end{vmatrix} = \begin{vmatrix} \cos\phi\sin\theta\cos\psi + \sin\phi\sin\psi \\ \cos\phi\sin\theta\sin\psi - \sin\phi\cos\psi \end{vmatrix} \tag{9}$$

where:

I_{xx}, I_{yy}, I_{zz} – four-rotor moment of inertia about the axis E_x, E_y, E_z,

l_a – the length of the four-rotor arm,

b, d - thrust, drag coefficient,

J_r - moment of inertia of the rotor about the axis of rotation,

m_s - total weight of the four-rotor,

g - acceleration due to gravity.

U is the input vector consisting of U_1 (total sequence), and U_2, U_3, U_4, which are related to the rotation of the quadrocopter, X is the state vector consisting of the following elements:

- translation components $\xi = [x, y, z]^T$ and their derivatives,
- rotating components i $\dot{\eta} = [\dot{\phi}, \dot{\theta}, \dot{\psi}]^T$ and their derivatives.

The effects of external disturbances were realized by introducing a vector of additional disturbances.

A nonlinear model is a set of equations (7), (8) and (9). These equations are represented as a simulation model in Matlab Simulink. The moment of resistance is neglected because the influence of these forces in the room is small compared to the thrust of a four-rotor.

The total angular velocity is Ω_r = 475 rad / s [14]. This angular velocity is the speed produced by the rotor used in the Parrot drone as specified in the Specifications. For the linearized model, an input impulse is given and the analysis is performed between the nonlinear and the linearized model. The design parameters of the model are given below:

- model weight, m = 2.5 kg,
- length of each arm, l = 0.122 m,
- vertical distance from the propeller center to the center of gravity, h = 0.005 m,
- radius of the propeller blade, r = 0.0635 m,
- inertia along the x and y axes, I_{xx} and I_{yy} = 5 * 10 - 3 kg / m 2,
- inertia along the z axis, I_{zz} = 10 * 10 - 3 kg / m 2,
- thrust factor, C_l = 1.5 Ns 2,
- drag coefficient, C_d = 1.3 Nms 2,
- angles at the linearization point = 0 rad / s.

Design parameters are substituted in matrices and a suitable nonlinear model for a given system is obtained.

The aim of the work is to build a usable mathematical model of a quadrocopter (QC) including actuators (UW) and to identify its parameters. The result of the work is the QC model taking into account the impact of changes in the design parameters of the four-rotor on the flight dynamics.

2. MATHEMATICAL DESCRIPTION OF PROPELLERS MOVEMENT

ILLUSTRATIONS

The dynamics of each engine to which the propellers of the quadrocopter are attached are described by the expressions [2]:

$$Q = K_q I \tag{10}$$

$$V = R_a I + K_e \omega \tag{11}$$

where:
Q - engine torque,
V - voltage on the engine,
I - current flowing through the engine,
ω - angular speed at which the engine rotates,
K_q - relationship of current to torque,
R_a - total resistance of the motor armature,
K_e - the dependence of the motor speed on the reverse value of the electromotive force.

The formula for power [15]:

$$P = IV \tag{12}$$

$$P = \frac{Q}{K_q} V \tag{13}$$

Equation (13) can be related to thrust by equating the power produced by the engine with the ideal power required to produce thrust by increasing air momentum. Ideally, the power is the thrust multiplied by the speed at which it is applied. In hover, this power P_h is [16]:

$$P_h = T\, V_h \tag{14}$$

where V_h is the hover induced velocity, i.e. the change in air velocity induced by the rotor blades with respect to the free jet velocity V_∞ [11]. We accept for analysis $V_\infty = 0$ hovering without wind. Using the results of the work [16]:

$$V_h = \sqrt{\frac{T}{2\rho A}} \tag{15}$$

T - thrust produced by the rotor to stay hovering,
A - πr^2 rotor reach area,
ρ - air density,
R - rotor radius,

For a four-rotor vessel, it is equal to - T_{nom}
T_{nom} - mass of the vehicle.

The torque is proportional to the thrust, with a constant K_t ratio, which depends on the rotor geometry [16].

$$Q = K_t T \tag{16}$$

The relationship between the applied voltage (V) and the thrust (T) can be found by equating the generated power (P) with the ideal energy consumed at hover (P_h) from equations (13) and (14) [16].

$$\frac{Q}{K_q} V = T V_h \tag{17}$$

$$\frac{Q}{K_q} V = T \sqrt{\frac{T}{2\rho A}} = \frac{T^{\frac{3}{2}}}{\sqrt{2\rho A}} \tag{18}$$

$$\frac{K_t T}{K_q} V = \frac{T^{\frac{3}{2}}}{\sqrt{2\rho A}} \tag{19}$$

$$T = \frac{2\rho A K_t^2}{K_\rho^2} V^2 \tag{20}$$

The thrust produced by the rotor is proportional to the square of the voltage applied to the motor. The total force F is given as [16]:

$$F = -D_b e_v + mg e_D + \sum_{i=1}^{4} (-T_i R_{R_i, I_b} Z_{R,i}) \tag{21}$$

where:

D_b - object resistance,

e_v - current speed unit vector,

m - object mass,

g - acceleration due to gravity,

e_D - unit vector along the vertical direction,

T_i - thrust generated by the i-th rotor,

$R_{Ri,Ib}$ - rotation matrix from the plane of the i-th rotor to the inertial coordinates,

$Z_{R,i}$ - axis of the rotor plane along which the thrust of the i-th rotor acts.

Similarly, the total moment M is [17]:

$$M = \sum_{i=1}^{4} (M_i + r_i(-T_i R_{R_i,B} Z_{R,i})) \quad (22)$$

where $R_{Ri,B}$ - rotation matrix from the plane of the rotor and to the coordinates of the body.

Note that D_b is ignored in the torque calculation. Since it was found that this force causes negligible disturbances in the moment, the full nonlinear dynamics can be described as [17]:

$$F = m\ddot{r} \quad (23)$$

$$M = I_b \dot{\omega}_B + \omega_B x I \omega_B \quad (24)$$

where ω_B - the angular velocity of the quadrocopter rotor along the fuselage frame.

The total moment is considered to be zero because the moments in the opposite pairs cancel each other when the position is fixed.

3. AERODYNAMIC EFFECTS

Equations of motion of a flying object, the steering of which takes place as a result of changes in three parameters: velocity and angles of tilt and deviation of the object velocity vector. The mathematical model of the quadrocopter was derived using the d'Albert dynamics equations for the rigid body. Some simplifications have been adopted in the modeling, e.g. aerodynamic drag forces are neglected. This simplification should not, however, significantly affect the quality of the model designed for the synthesis of the spatial orientation control system, as these forces near the steady hover state are relatively small. Moreover, it is practically difficult to determine or verify their value.

While vehicle dynamics are accurately linearly modeled for position and altitude control, this is only acceptable at low speed. Even at low speed, the influence of aerodynamic effects resulting from changes in air speed is significant [10].

There are four main effects, three of which are quantifiable and incorporated into the non-linear vehicle model for estimation and control purposes. The second, which causes irregular air flow and therefore can be alleviated by redesigning the structure [10]. The types of aerodynamic effects are irregular airflow, total thrust, inflow velocity, flutter and irregular thrust [18].

The total thrust varies not only with the power input, but also with the free stream velocity and angle of attack relative to the free stream. This is complicated by a flight state, called the vortex ring state, where there is no analytical solution for thrust, and experimental data show that thrust is random. Induced power is the required input power to produce the induced speed. When the rotorcraft is in transition or changes its angle of attack, the induced power requirement changes [11].

In order to obtain the effect of the free flux velocity on the induced power, the induced speed V_i is obtained by solving the following equation [19]:

$$T = \frac{V_h^2}{\sqrt{(V_\infty \cos\alpha)^2 + (V_\infty \sin\alpha + V_i)^2}} \quad (25)$$

where:

V_∞ - total free jet speed, including translational speed and ambient wind speed,

α - angle of attack; positive - forward tilt.

This equation is less accurate for a high rake angle and is not correct during a vortex ring condition. Nevertheless, it provides an accurate result for most useful flight conditions.

Using V_i, it is possible to calculate the ideal string for the input power [19]:

$$T = \frac{P}{V_\infty \sin\alpha + V_i} \quad (26)$$

The denominator corresponds to the air velocity across the rotor. At low speed, α has little effect on T / Th.

As in airplanes, increasing the angle of attack increases the lift [10]. In level flight, the power required to maintain altitude increases with the forward speed. In the extreme area α, where the flight is close to vertical, the rotor has three operating modes for the climb speed V_c [19]:

- nominal working condition $0 \leq \frac{V_c}{V_h}$,
- the state of autorotation $\frac{V_c}{V_h} < -2$,

– swirl ring condition $-2 \leq \frac{V_c}{V_h} < 0$.

In normal operating condition, air flows through the impeller. In the autorotating state, air flows through the rotor due to the rapid sinking. For these two states, the conservation of momentum can be used to obtain induced velocity.

For a normal state [19]:

$$V_i = -\frac{V_c}{2} + \sqrt{\left(\frac{V_c}{2h}\right)^2 + {V_h}^2} \quad (27)$$

For the autorotation state [19]:

$$V_i = -\frac{V_c}{2} - \sqrt{\left(\frac{V_c}{2h}\right)^2 - {V_h}^2} \quad (28)$$

In the annular vortex state, air circulates through the blades periodically and somewhat randomly. As a result, the induced speed varies significantly, especially in the $-1{,}4 \leq V_c/V_h < 0{,}4$ range, reducing the aerodynamic damping. The empirical model of the velocity induced in the ring vortex state is [19-21]:

$$V_i = -V_h\left(K + K_1\left(\frac{V_c}{V_h}\right) + K_1\left(\frac{V_c}{V_h}\right) + K_2\left(\frac{V_c}{V_h}\right)^2 + K_3\left(\frac{V_c}{V_h}\right)^3 + K_4\left(\frac{V_c}{V_h}\right)^4\right) \quad (29)$$

where:

$K_1 = -1{,}125$; $K_2 = -1{,}372$; $K_3 = -1{,}718$; $K_4 = -0{,}655$

To model the dynamics during a climb, power is the thrust multiplied by the velocity with which it is applied [20]:

$$T = \frac{P}{V_c + V_i} \quad (30)$$

where:

$T*V_c$ - power absorbed by the climbing movement,

$T * V_i$ - power transferred to the air.

In further mathematical considerations with regard to the simulation tests, the forces generated on each of the four wing profiles in the four-rotor were ignored, which would allow to avoid eddy air streams, while maintaining a significant forward speed during descent to landing.

4. RESULTS FROM SIMULATION TESTS

The quadrocopter should respond to the operator's commands, which will indicate at what height it is to be, in which direction it should move and whether it should turn. By converting these data together with information from measuring devices, the control system generates rotational speed values for motors. This signal goes to the engine regulators. The control was performed by a PID controller. The proportional part P has a direct influence on the gain, so it is responsible for the oscillations of the quadrocopter and its overshoots. The integral part eliminates imperfections in the vehicle (e.g. inaccurate balancing, engine and propeller losses). By selecting appropriate values of the derivative term D, it is possible to counteract rapid changes in the object deflection angle. A test platform was prepared that did not allow the quadrocopter to fly, but at the same time allowed it to rotate in one axis. This made it possible to conduct safe experimental tests of the regulator settings selection. Finally, Kp = 1 was obtained.

In computer tests aimed at assessing the dynamics of the quadruple rotor during flight, the values characterizing the selected regulator should be appropriately selected. In the case under consideration, the PID controller was selected from the value of Ki = 0.3 so that the tested object would show adequate performance in terms of the aerodynamic force value. In particular, the Ki parameter should be properly selected so that there is no imbalance during the unmanned aerial vehicle flight. The occurring mild permanent oscillations of the aircraft and the large effect of the flight balance disturbance resulted in larger oscillations, which led to the destabilization of the system. The frame on which the engines are mounted are defined rectangularly to the Earth, i.e. with the gravity in the negative *Z* direction. The vectors of the unmanned aerial vehicle fuselage frame describing the linear and angular positions of the quadrocopter are usually represented as: translational speeds $[u,v,w]^T$ and rotational speeds $[p,q,r]^T$. In turn, the inertial system is defined by the orientation of the quadrcopter with the rotor axes directed in the positive direction z and the arms directed in the *X* and *Y* directions. Within this system, the position is determined $[x,y,z]$ (roll, pitch and yaw) and greatness $[\phi,\theta,\psi]$ describe its linear and angular position. The combination of these four vectors defined on the fuselage and the inertial frame represents 24 dynamic states during the four-rotor motion. According to the work [1], four-rotor ships are described by non-linear equations and are modeled with the following assumptions. It is a helicopter with 24 dynamic

states (six altitude states and six positions and linear velocities on each of the four rotors), and the object is characterized by 6 degrees of freedom (3 speeds for three different linear and rotational motion variables). It is started by four independent rotors. The conclusion from this description by various researchers is that the dynamics of the quadripotron is highly mismatched and highly nonlinear, burdened with irregular aerodynamic uncertainties (because four rotors are used to control the helicopter). The further part of the article presents the results of tests carried out in Matlab software. Figures 2 and 3 show, respectively, the course of rotary motion and the position of the tested UAV object in a rectangular coordinate system. It can be noticed that the greatest fluctuations in the rotational movement responsible for the height, which after reaching about 90 meters above sea level, were maintained without major disturbances. The rotary motion for the x and y directions was characterized by slight disturbances resulting from the maneuver of raising and turning the unmanned aerial vehicle. The values for both directions oscillated around 4 meters.

Subsequently, roll and pitch simulations were carried out. While quadrcopter are capable of many forms of motion, most literature and publications focus mainly on the following motions: yaw motion corresponds to the rotation of the quadrcopter about the Z axis. It is produced by the difference in torque produced by each pair of rotors; one pair produces torque in a clockwise direction and the other in a counterclockwise direction. By changing the angular velocity of one pair to the other, the net torque applied to the helicopter generates the yawning motion. Positive bias is achieved by setting ($\omega_1 = \omega_3$)>ω and ($\omega_2 = \omega_4$) < ω. Negative deviation is obtained by setting ($\omega_1 = \omega_3$)< ω_{hover} and ($\omega_2 = \omega_4$) > ω_{hover}. This situation is presented in Fig. 4.

Pitch-motion corresponds to the rotation of the quadrcopter on the Y axis is obtained when $\omega_1=\omega_3=\omega$ will hang and ω_2 and ω_4 will be changed. For a positive jump, ω_2 >ω goes up and i ω_4 < ω goes up, while a negative jump is obtained when ω_2 < ω goes up and ω_4 > ω goes up. The results of the motion are presented in Fig. 5. Roll-motion is responsible for the rotation of the quadrcopter along the X axis. It is obtained when $\omega_2=\omega_4=\omega$ will hang and ω_1 and ω_3 will be changed. For a positive roll ω_1 > ω go up and ω_3 < ω go up. Negative rotation occurs when we put ω_1 < ω at the hinge and ω_3 > ω at the hinge. The parameter $\omega_{1,2,3,4}$ is the rotational speed on motors 1 to 4. This situation is shown in Fig. 6.

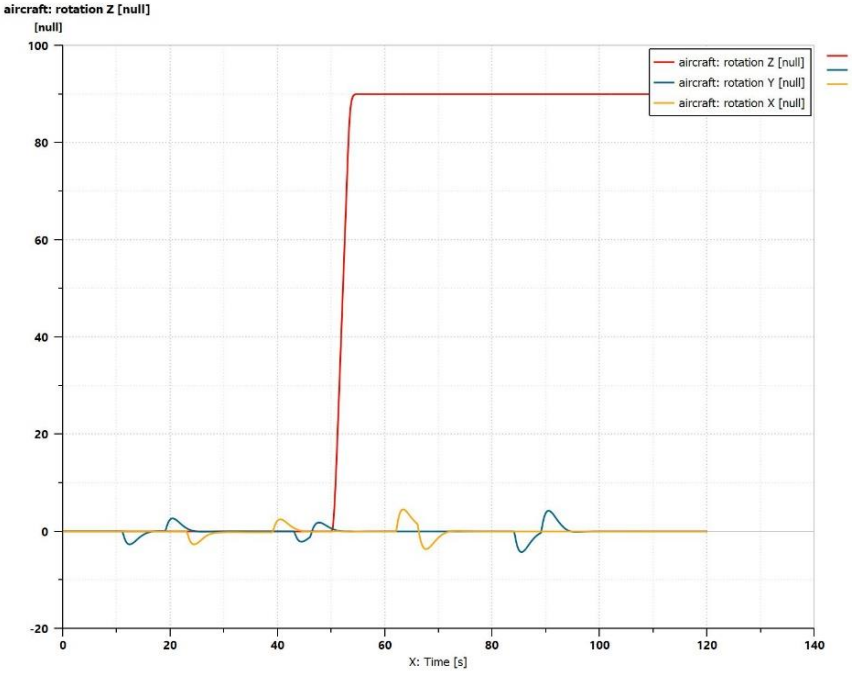

Fig. 2. Waveforms of the rotational motion of a quadrocopter object during flight

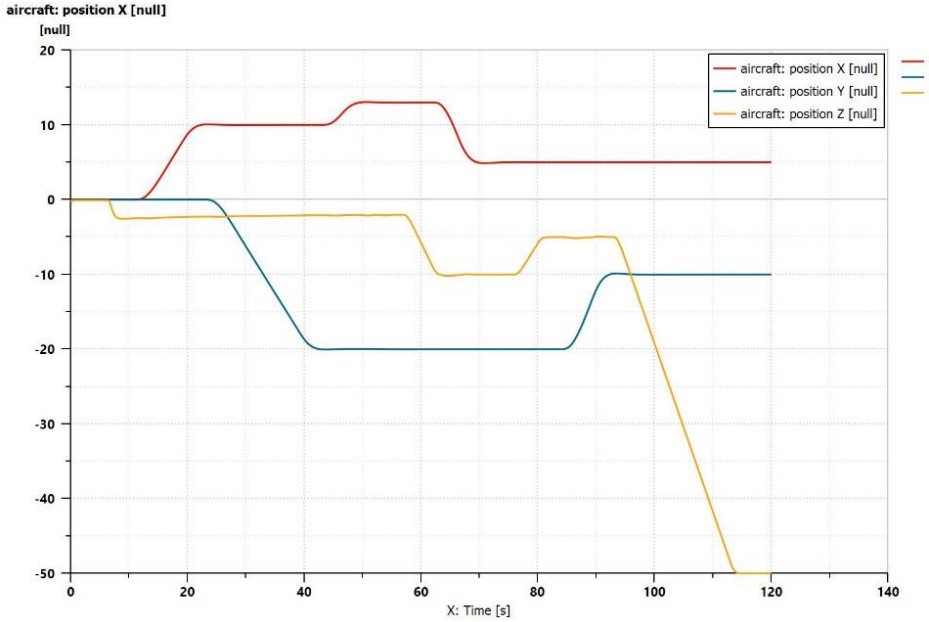

Fig. 3. Location of the UAV object in the xyz coordinate system

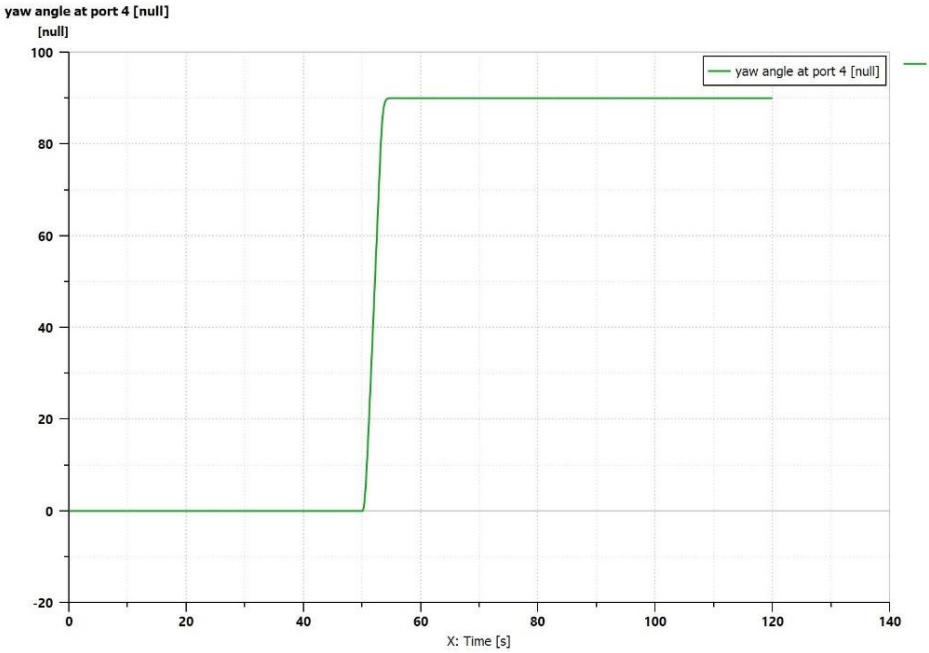

Fig. 4. Yaw tilt of the UAV facility during flight

The change in the yaw angle is visible while the quadrocopter is climbing to a certain height and it stops at a constant value of about 90 meters.

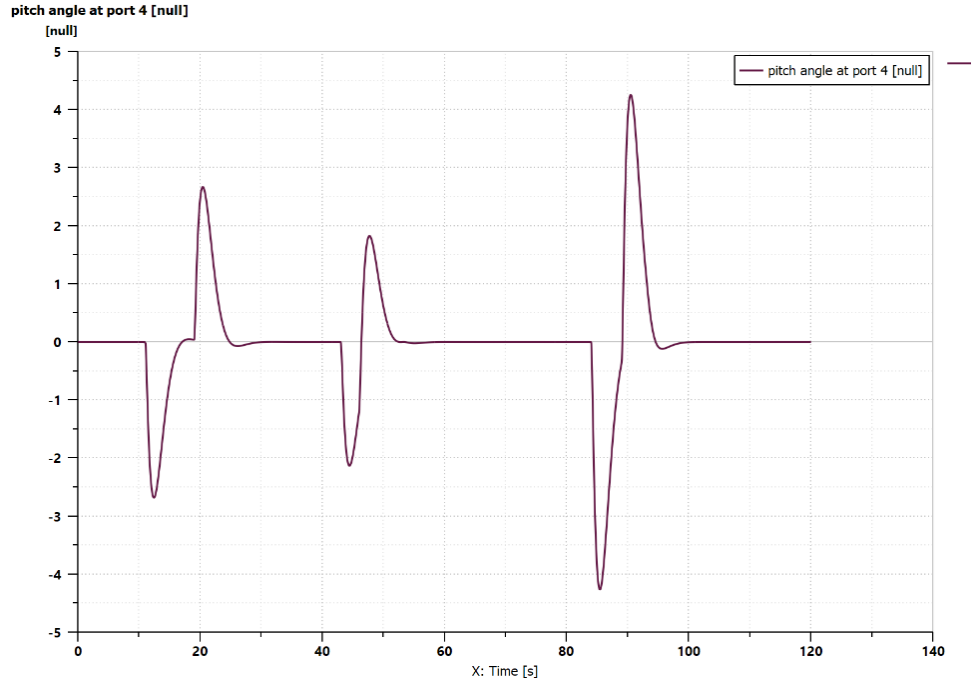

Fig. 5. The pitch deviation of the UAV object during flight

The pitch angle fluctuations during the change of the flight direction were within about 8 meters, which will translate into disturbances during the course control (right or left).

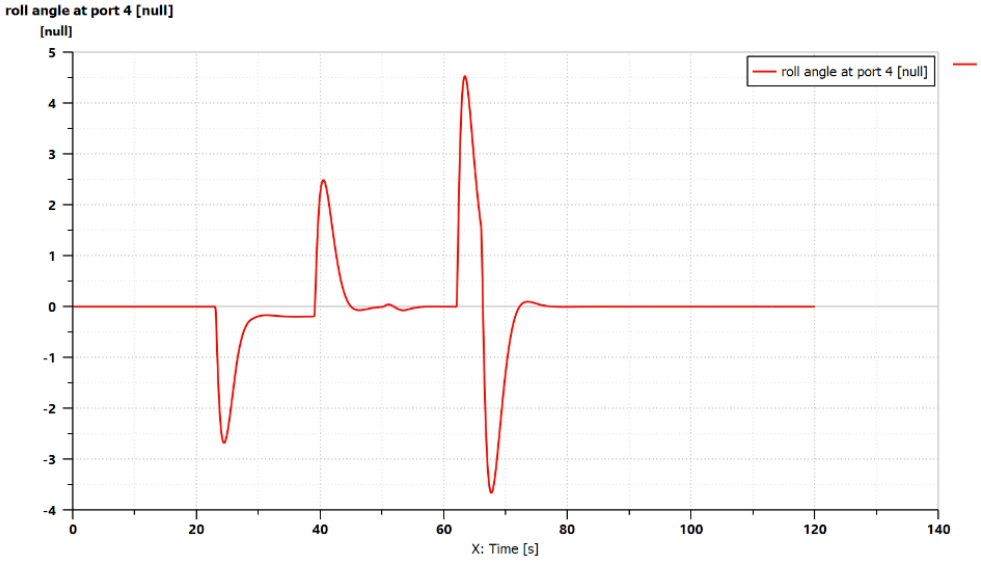

Fig. 6. The roll slope of the UAV object during the flight

The same is the case for the roll angle, the range of which is within 8 meters.

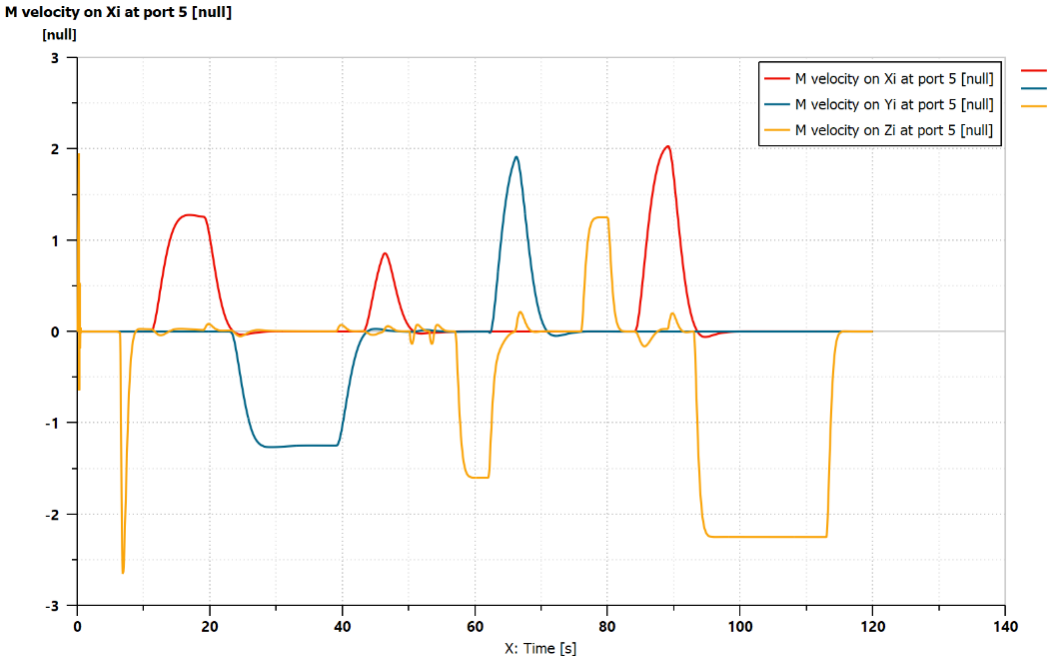

Fig. 7. Change of the torque speed of the UAV object during flight

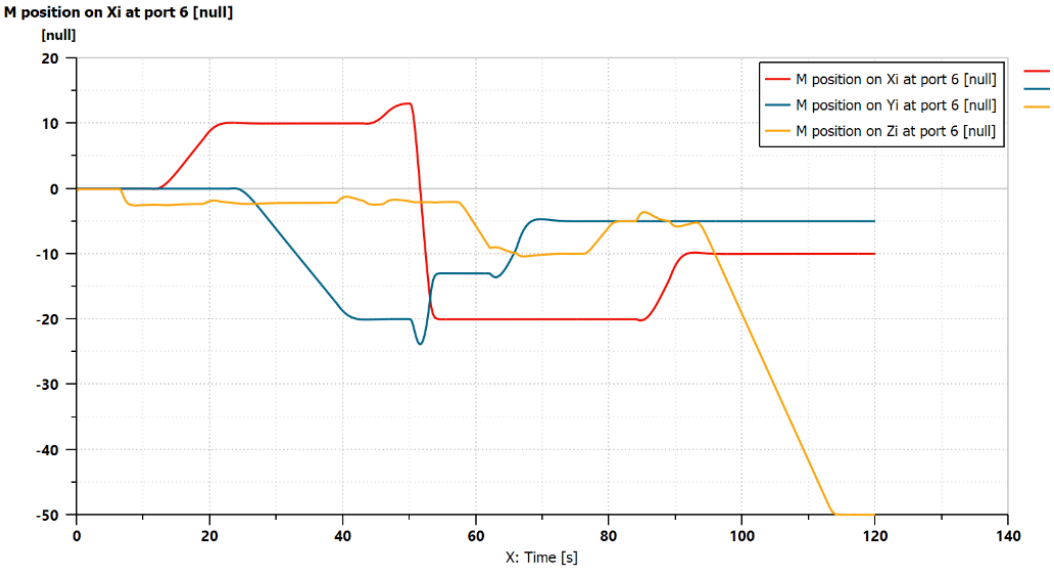

Fig. 8. Changing the position of the UAV torque

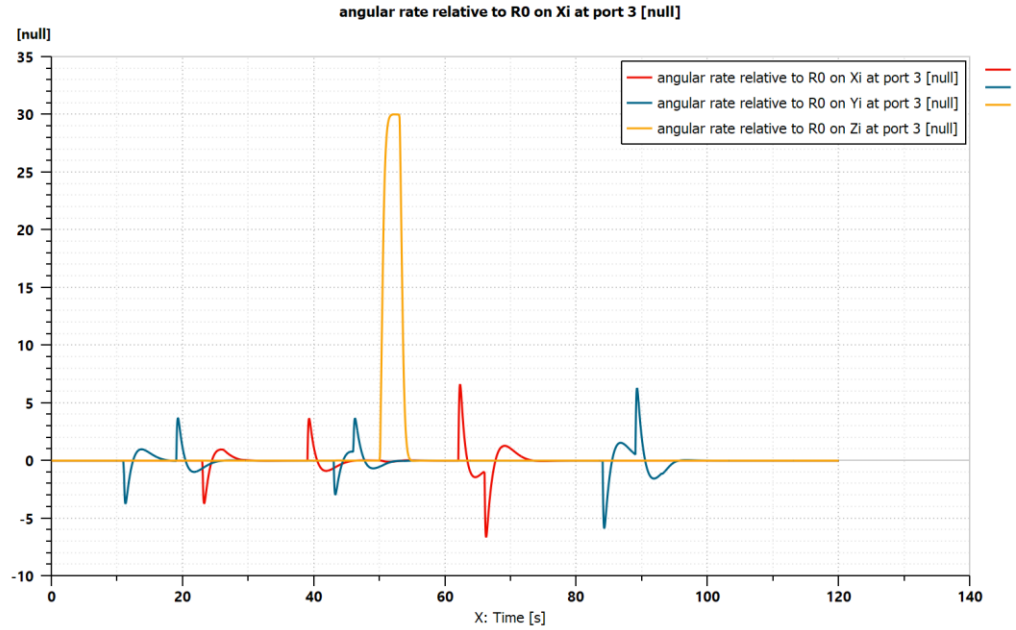

Fig. 9. Change of the UAV's rotation angle during the flight

Figures 7-9 show the changes in speed, torque position and rotational angle.

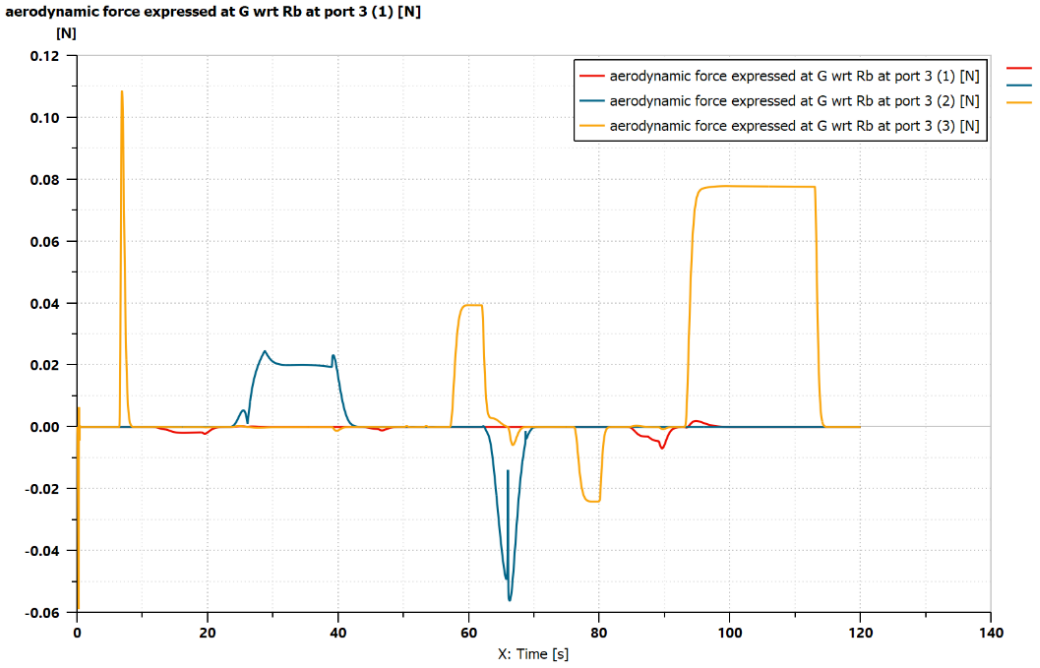

Fig. 10. Aerodynamic forces occurring during the UAV flight

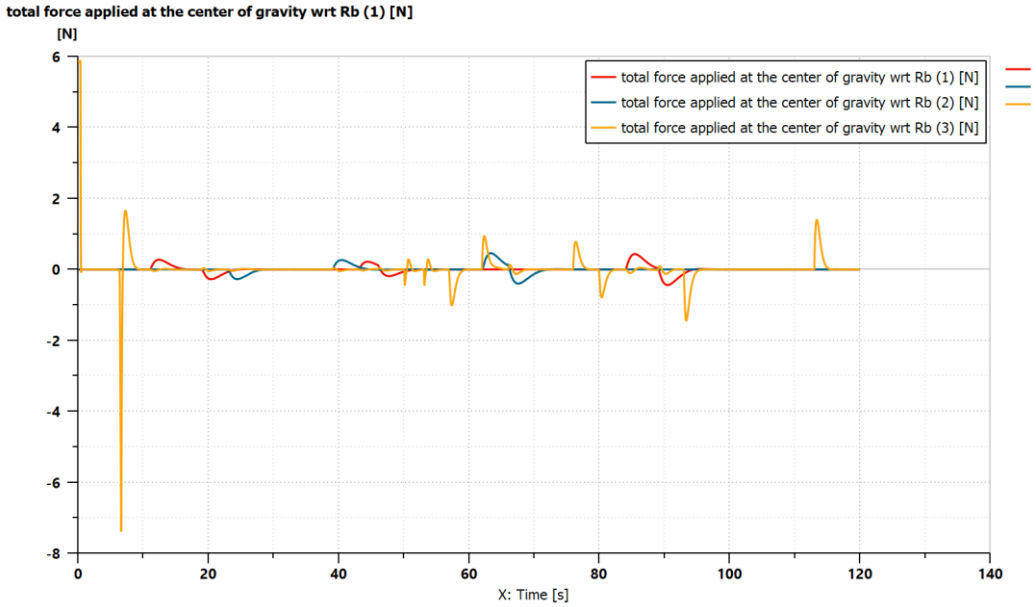

Fig. 11. Forces occurring in the center of gravity of the UAV during the flight

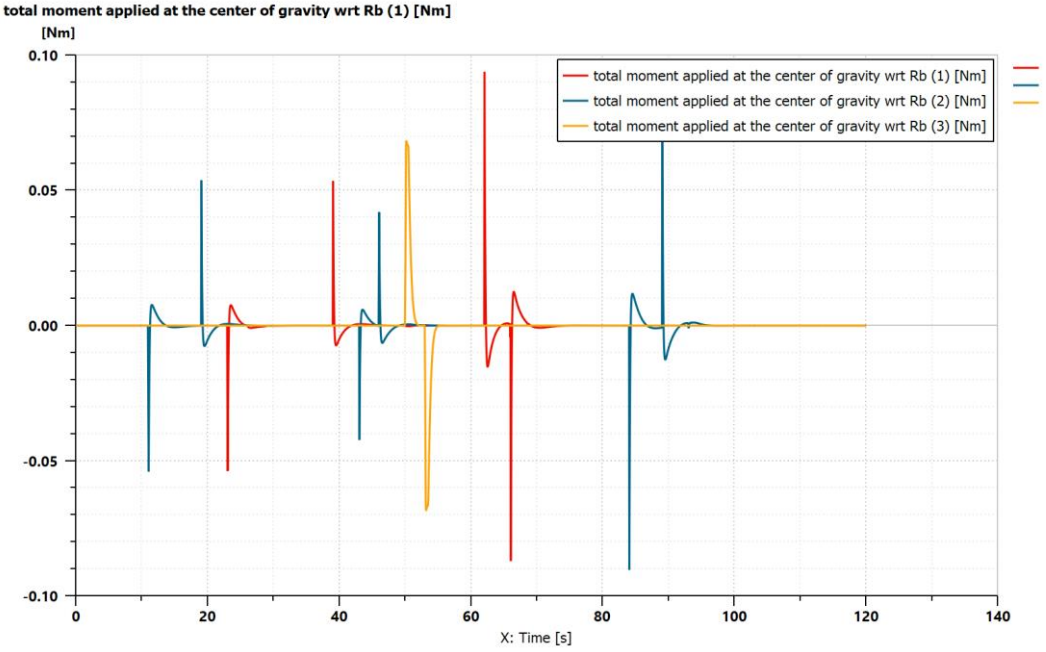

Fig. 12. Moments in the center of gravity of the UAV during the flight

Figures 10 to 12 show the forces and moments occurring during the flight. The presented diagrams show that the forces on the rotors and the moments varying from the rotational speed of the motion and the direction of flight in the three axes x, y and z have been compared.

CONCLUSIONS

Nowadays, drones are gaining more and more popularity due to their trouble-free movement in places inaccessible to people and their increasing use by amateurs. The article describes the design and steps leading to the DIY quadrocopter, which is perfect for research and industrial applications. All the above-mentioned design assumptions have been met, the quadrocopter flight is smooth and can stabilize its position by itself. The article presents the design and construction of a quadrocopter flying platform. Its flexibility, resulting from the modular structure, allows for simple modification and expansion. In the near future, it is planned to develop and implement more effective, more advanced control algorithms in the vehicle. The developed mathematical model of the four-rotor, after it was linearized, was used to design the spatial orientation control system. Positive results of simulation tests suggest that this system will fulfill its task also in real conditions. Existing control algorithms can be expanded with superior systems that control altitude, position and flight trajectory, while aiming at full autonomy of the aircraft. The obtained waveforms of the controlled values have the desired dynamic properties and are mutually independent, despite the existing cross-couplings in the system.

MODELOWANIE MATEMATYCZNE RUCHU BEZZAŁOGOWEGO STATKU POWIETRZNEGO - CZTEROWIRNIKOWIECA

W artykule przedstawiono analityczne podejście do budowy modelu matematycznego czterowirnikowca. Głównym celem budowy modelu było zaprojektowanie odpowiedniego systemu sterowania obiektem oraz analiza jego zachowania w różnych sytuacjach. Przyjęto założenie, aby model, system sterowania oraz wszystkie towarzyszące im algorytmy zbudować w otwartym środowisku programistycznym, co pozwoli na ich późniejszą implementację w rzeczywistym obiekcie, bez konieczności stosowania drogiego oprogramowania. Sterowanie czterowirnikowcem przez operatora odbywa się za pomocą ruchów ręki, które są odczytywane przez kamerę i odpowiednio interpretowane przy użyciu zaawansowanych metod przetwarzania obrazu. Cały system jest wizualizowany i osadzony w trójwymiarowym środowisku symulacyjnym. Badania modelowe przeprowadzono z wykorzystaniem silnika prądu stałego jako źródła danych wejściowych. Działanie modelu zostało sprawdzone za pomocą kontrolera po wprowadzeniu do modelu zakłócenia. Model czterowirnikowca z wybranym regulatorem testowano analizując prędkość kątową i położenie obiektu w prostokątnym układzie współrzędnych. Na końcu artykułu zaprezentowano wyniki przeprowadzonych symulacji oraz przedstawiono wynikające z nich wnioski.

Słowa kluczowe: czterowinikowiec, model matematyczny, dynamika, sterowanie, bezzałogowy statek powietrzny

REFERENCES

[1] Leishman J.G. (2000) Principles of Helicopter Aerosynamics. New York, NY: Cambridge University Press; 2nd edition (December 15, 2016), ISBN 1107013356
[2] Alexis K., Nikolakopoulos G. Tzes A., (2012) "Model Predictive quadrotor control: attitude, altitude and position experimental studies". IET Control Theory Appl., 12, pp. 1–16. https://doi.org/10.1049/iet-cta.2011.0348
[3] Phillips, W. F. (2004) Mechanics of Flight, J. Wiley&Sons, ISBN 9780470539750
[4] Schmidt, D. (2012) Modern Flight Dynamics. McGraw-Hill, ISBN 007339811X
[5] Kisilowski J. (1978) Dynamics of the track-vehicle system. ITPW Studies, Issue 15, Warsaw
[6] Kisilowski J. (ed.) (1991) Dynamics of the Mechanical System, Rail Vehicle-Track, PWN, Warsaw
[7] Bouadi H., Tadjine M. (2007) "Nonlinear observer design and sliding mode control of four rotors helicopter". Proceedings of World Academy of Science, Engineering and Technology, vol. 25, pp. 225–230. https://doi.org/10.5281/zenodo.1055781
[8] Leonov G.A., Kuznetsov N.V. (2007) "Time-Varying Linearization and the Perron effects". International Journal of Bifurcation and Chaos, 17(3). https://doi.org/10.1142/S0218127407017732
[9] Mathworks, Simulink Getting Started Tutorial
[10] Maryniak J. (ed.) (1992) Mechanics in aviation. Polish Society of Theoretical and Applied Mechanics
[11] Maryniak J. (ed.) (2006) Mechanics in Aviation ML-XII 2006, Polish Society of Theoretical and Applied Mechanics, ISBN 83-902194-6-8
[12] Bouabdallah S., Siegwart R. (2007) "Full control of a Quadrotor". Intelligent Robots and Systems. https://doi.org/10.1109/IROS.2007.4399042
[13] Bouabdallah S., P. Murrieri P., Siegwart R. (2004) "Design and control of an indoor micro quadrotor". IEEE International Conference on Robotics and Automation. Proceedings. ICRA '04.2004, New Orleans, LA, USA. https://doi.org/10.1109/ROBOT.2004.1302409
[14] https://en.wikibooks.org/wiki/Control_Systems/Controllability_and_Observability (access date: 14/09/2020)

[15] Defence Research and Development Organisation. Dynamic Modelling of DC Motor and Simulation, Chandipur, India.
[16] Cook M. (2007) Flight Dynamics Principles. Elsevier, ISBN 9780080982427
[17] Ashley, H. (1974) Engineering Analysis of Flight Vehicles. Addison-Wesley, ISBN 9780486672137
[18] http://ritzel.siu.edu/courses/302s/vehicle/vehicledynamics.html (access date: 17/09/2020)
[19] Huang H., Hoffmann G. M., Waslander S. L., Tomlin C. J. (2009) "Aerodynamics and control of autonomous quadrotor helicopters in aggressive maneuvering". IEEE International Conference on Robotics and Automation, pp. 3277–3282. https://doi.org/10.1109/ROBOT.2009.5152561
[20] Beard R. (2008) "Quadrotor dynamics and control rev 0.1"
[21] Ažaltovič, V., Škvareková, I., Pecho, P., Kandera, B. (2020) "Calculation of the ground casualty risk during aerial work of unmanned aerial vehicles in the urban environment". Transportation Research Procedia, 44, pp. 271-275. https://doi.org/doi:10.1016/j.trpro.2020.02.043
[22] Pecho, P., Ažaltovič, V., Kandera, B., & Bugaj, M. (2019) "Introduction study of design and layout of UAVs 3D printed wings in relation to optimal lightweight and load distribution". Transportation Research Procedia, 40, pp. 861-868. https://doi.org/doi:10.1016/j.trpro.2019.07.121